The Reflectance Spectra of $(BEDT\text{-}TTF)_5Hg_3Br_{11}$ and $(BEDT\text{-}TTF)HgBr_3$. The Estimation of Effective On-Site Coulomb Interaction

Hiroyuki TAJIMA,* Masafumi TAMURA, Haruo KURODA, Takehiko MORI,† and Hiroo INOKUCHI†
Department of Chemistry, Faculty of Science, The University of Tokyo, Hongo, Tokyo 113
†Institute for Molecular Science, Okazaki, Aichi 444
(Received September 7, 1989)

The reflectance spectra of $(BEDT\text{-}TTF)_5Hg_3Br_{11}$ and $(BEDT\text{-}TTF)HgBr_3$ were measured by using the microspectrophotometric technique in the spectral range from 450 cm^{-1} to 25000 cm^{-1}. In the former salt, the gap formation due to a metal-insulator transition was observed in the reflectance spectrum at 100 K. In the latter salt, the effective Coulomb interaction and the intra-dimer transfer integral were estimated and compared with the corresponding values of BMDT-TTF and TTF.

In the past several years a variety of charge-transfer (CT) salts of BEDT-TTF and their derivatives have been synthesized, and their structures and physical properties have been extensively investigated. Several salts of this group have been found to behave as organic superconductors.[1] Simple band calculations based on the Extended Hückel method were recently carried on some of these CT salts, and the experimentally determined band parameters were compared with the calculated band structures.[2-4] Optical measurement provides important information concerning the band structures of these organic solids. The results of our previous optical study of a series of BEDT-TTF salts suggested the existence of two different types.[5] The first is the type whose optical properties can be roughly understood in terms of the simple band model. κ-$(BEDT\text{-}TTF)_2I_3$, β-$(BEDT\text{-}TTF)_2I_3$, θ-$(BEDT\text{-}TTF)_2I_3$ and, β''-$(BEDT\text{-}TTF)_2ICl_2$ belong to this type. Hereafter we will denote this as the "A-type". Most of the A-type salts show metallic properties. The second is the type whose optical properties can not be understood within the framework of the simple band theory. Most of them are semiconductors. β'-$(BEDT\text{-}TTF)_2ICl_2$ is an example of this type, which we will call as "B-type". Some of the typical one-dimensional organic conductors, involving other donors such as TMTTF, also belong to this type.[6] The electron-electron correlation seems to play an important role in this type of salt.

A similar classification has also been proposed by Mazumdar et al.[7] Before the finding of BEDT-TTF salts, it was not easy to obtain clear-cut experimental evidence to show whether the effects of Coulomb interactions were large or small in comparison with the widths of the bands. The family of BEDT-TTF salts is unique in this respect, since the two different types commonly exist in one family. This character may originate from the reduction of the electron-electron interaction due to the expansion of π-HOMO and from the increase in dimensionality due to the intermolecular S-S interaction.[8] The degree of charge-transfer and the existence of two-dimensional interaction seems to be a factor strongly affecting whether a BEDT-TTF salt becomes A-type or B-type. Therefore, it is of great interest to compare the optical properties of the BEDT-TTF salts which are mutually different in the degree of charge-transfer and in the crystal structure. We will report in this paper a reflectance-spectrum study of $(BEDT\text{-}TTF)_5Hg_3Br_{11}$ and $(BEDT\text{-}TTF)HgBr_3$, both of which have a unique crystal structure containing mercury bromide. $(BEDT\text{-}TTF)_5Hg_3Br_{11}$[9] is a A-type salt with a semimetallic band structure, including $BEDT\text{-}TTF^{4/7+}$; it exhibits a metal-insulator transition at 120 K. $(BEDT\text{-}TTF)HgBr_3$[9] is a B-type salt including $BEDT\text{-}TTF^{+}$ with a strongly dimerized structure. For the latter salt, we shall estimate the effective Coulomb interaction (U_{eff}) by the use of the dimer model. This is the first estimation of U_{eff} in a simple salt of BEDT-TTF with a dimerized structure.

Experimental

Single crystals of $(BEDT\text{-}TTF)_5Hg_3Br_{11}$ and $(BEDT\text{-}TTF)HgBr_3$ were electrochemically obtained from a benzonitrile solution by the use of $(Et_4N)_2HgBr_4$ and $(Me_4N)HgBr_3$ respectively as electrolytes.[9] The typical sizes of the crystal used in the optical measurement were 2.0 mm×0.4 mm×0.03 mm for $(BEDT\text{-}TTF)_5Hg_3Br_{11}$ and 1.4 mm×0.2 mm×0.03 mm for $(BEDT\text{-}TTF)HgBr_3$. The reflectance spectra were measured by the use of Olympus MMSP microspectrophotometer from 4200 cm^{-1} to 25000 cm^{-1} and with a Jasco MIR 300 microspectrophotometer from 450 cm^{-1} to 4200 cm^{-1}. The temperature control was achieved by the use of a closed cycle cryogenic refrigerator manufactured by CTi SPECTRIM^{tm} for the visible spectrometer and by the use of a continuous flow helium cryostat manufactured by Oxford Instruments respectively. The details of these apparatuses have been described elsewhere.[3a,10,11] The crystal face and the crystal axes of the sample were determined by the use of the X-ray diffraction technique.

Results and Discussion

$(BEDT\text{-}TTF)_5Hg_3Br_{11}$. The ten BEDT-TTF molecules in the unit cell of this salt can be divided into two groups.[9] The three BEDT-TTF molecules holding a 2+ charge are sandwiched by the anion sheets.

The rest of the BEDT-TTF molecules, holding a 4/7+ charge, form a chain along the [$\bar{1}$02] axis. The conduction path is formed mainly through the latter group of BEDT-TTF molecules. According to the simple band picture, this material can be expected to have a semimetallic band structure. The reflectance spectra were measured on the ac-plane for the light polarization along the optical axes, which were themselves determined by rotating the polarizer at 3300 cm^{-1}. By the X-ray diffraction, the optical axes thus determined were found to be parallel and perpendicular to [$\bar{1}$02], i.e. parallel and perpendicular to the chain direction of BEDT-$TTF^{4/7+}$.

Figure 1 shows the temperature dependence of the reflectance spectra. Although the maximum dispersion is found for the light polarization along the [$\bar{1}$02] direction, a weak dispersion is also found for the other polarization. This weak dispersion clearly indicates the existence of a significant interchain interaction, as is usually found in BEDT-TTF salts. The infrared broad dispersions, appearing for both polarizations, can be ascribed to the inter-band transition overlapping with the intra-band transition. This interpretation is the same as that which we have previously reported for the reflectance spectra of semimetallic BEDT-TTF salts.[12,13] The outstanding peak at 12000 cm^{-1} in the //[$\bar{1}$02] spectrum is attributable to the local excitation of BEDT-TTF^{2+}. The excitation energy of this transition is higher by about 1000 cm^{-1} than that of the corresponding transition of BEDT-$TTF^{\rho+}$ ($0<\rho<1$). This dispersion appears strongly in the //[$\bar{1}$02] spectrum, because the long axis of BEDT-TTF^{2+} has a large component along the [$\bar{1}$02] axis.[14]

This salt is known to become an insulator at 120 K.[9] The reflectivity below 1000 cm^{-1} decreases for both polarization when the phase transition takes place. This phenomenon is ascribed to the gap formation associated with metal-insulator transition. On the contrary, the reflectance spectra near the plasma edge does not change below and above the transition temperature. This result is markedly different from what has been observed in other BEDT-TTF salts. A hump does appear at the plasma-edge region on going to the insulator phase in the cases of α-(BEDT-$TTF)_3(ReO_4)_2$,[13] and α-(BEDT-$TTF)_2I_3$,[13] and a gradual increase in reflectivity near the plasma edge was observed below the transition temperature in the case

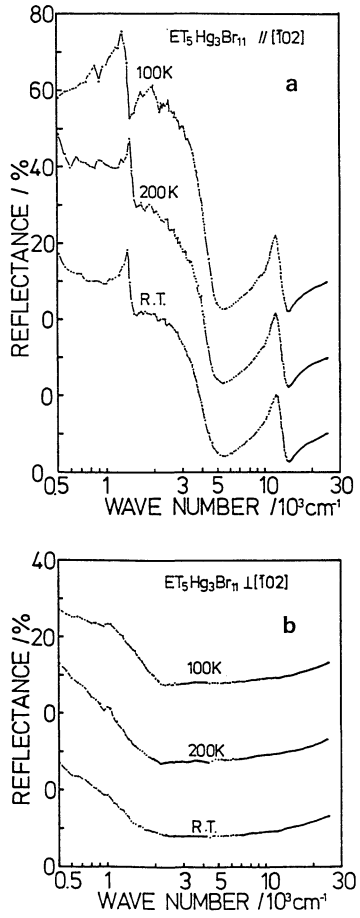

Fig. 1. Temperature dependence of the reflectance spectra of $(BEDT\text{-}TTF)_5Hg_3Br_{11}$ for the polarization (a) parallel and (b) perpendicular to the [$\bar{1}$02] axis.

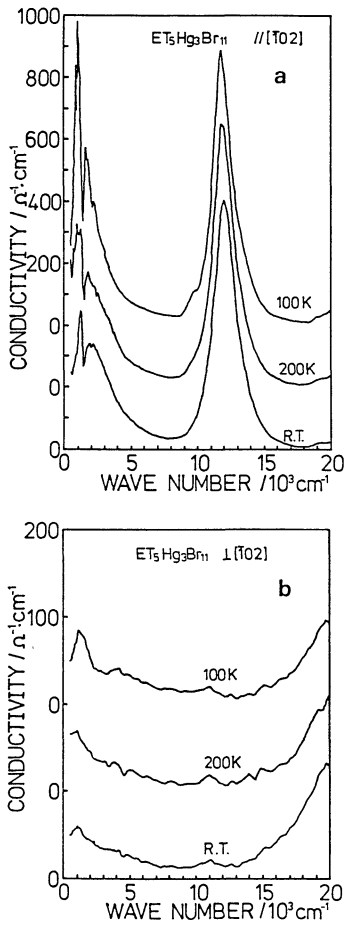

Fig. 2. Temperature dependence of the conductivity spectra of $(BEDT\text{-}TTF)_5Hg_3Br_{11}$ for the polarization (a) parallel and (b) perpendicular to the [$\bar{1}$02] axis.

of (BEDT-TTF)$_3$(ClO$_4$)$_2$.[12] Figure 2 shows the frequency-dependent conductivity obtained through the Kramers-Kronig transformation of the reflectance spectra shown in Fig. 1. Although three types of interpolation were made in the Kramers-Kronig analysis, the resulting spectra were little affected by the choice of interpolation. In the spectrum at 100 K, the conductivity sharply decreases at the low-wavenumber limit of the spectrum. This is likely to be associated with the appearance of a band gap, which is reported to be 0.06 eV (480 cm^{-1}) from the d.c.-conductivity measurement.[9]

By integrating the conductivity spectra from the zero wave number to 8000 cm^{-1}, we calculated the plasma frequency, ω_{pi} (i=1 or 2), by the use of the following equation:

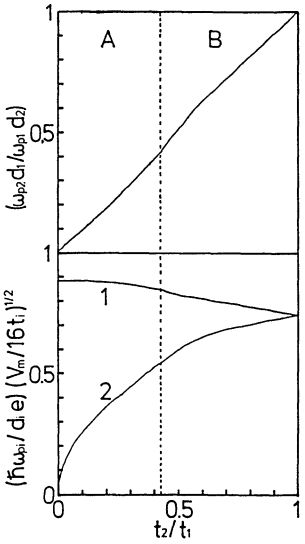

Fig. 3. Relation between the plasma frequencies (ω_{p1}, ω_{p2}) and the transfer integrals (t_1, t_2) in the orthorhombic two-dimensional two-sevenths (or five-sevenths) filled tight-binding model. The dotted line denotes the boundary between the open (A) and closed (B) Fermi surface. The bottom graphs show normalized plasma frequencies, i.e. $(\hbar\omega_{pi}/d_ie)(V_m/16t_i)^{1/2}$ (i=1, 2). V_m, d_1, and d_2 are the volume per BEDT-TTF$^{4/7+}$ molecule, the distance between adjacent BEDT-TTF$^{4/7+}$ within the chain, and the distance between adjacent chains of BEDT-TTF$^{4/7+}$ within the conducting sheet, respectively.

Table 1. The Mean Transfer Integral and Plasma Frequency of (BEDT-TTF)$_5$Hg$_3$Br$_{11}$ and Several Organic Conductors

	(BEDT-TTF)$_5$Hg$_3$Br$_{11}$			(1)	(2)	(3)
	R.T.	200 K	100 K	R.T.	R.T.	R.T.
ω_{p1}/eV	0.91	0.96	0.99	1.30	1.18	1.39
t_1/eV	0.17	0.19	0.20	0.12	0.12	0.25
ω_{p2}/eV	0.38	0.40	0.42	0.55	0.60	0.29
t_2/eV	0.06	0.06	0.07	0.07	0.08	0.03
t_2/t_1		ca. 0.3		ca. 0.6	ca. 0.7	ca. 0.1

(1): (BEDT-TTF)$_3$(ClO$_4$)$_2$,[12] (2): (BEDT-TTF)$_3$(ReO$_4$)$_2$,[13]
(3): (TMTSF)$_2$PF$_6$.[16]

$$\omega_{pi}^2 = 8\int\sigma_i(\omega)d\omega, \quad (1)$$

where the subscript (i=1 or 2) represents the direction either parallel or perpendicular to the stacking axis. In order to estimate the anisotropy from the plasma frequencies, we assumed the simple band structure expressed by

$$E(k_1, k_2) = -2t_1\cos(k_1d_1) - 2t_2\cos(k_2d_2). \quad (2)$$

This model is based on the orthorhombic lattice, where the lattice constants, d_1 and d_2, are the distance, between adjacent BEDT-TTF$^{4/7+}$ within the chain and the distance between adjacent chains of BEDT-TTF$^{4/7+}$ within the conducting sheet respectively. The corresponding transfer integrals, t_1 and t_2, may be considered to be weighted averages of several transfer integrals in the correct triclinic band structure. By virtue of this simplification, the values of ω_{p1} and ω_{p2} were numerically calculated from t_1 and t_2 by the use of the Lindhard equation.[15] Figure 3 shows the results of numerical calculation on the relation between (ω_{p1}, ω_{p2}) and (t_1, t_2). By the use of this figure and these parameters, d_1=4.32 Å, d_2=6.20 Å, and V_m (the volume per BEDT-TTF$^{4/7+}$)=655 Å^3, the effective transfer integrals (t_1, t_2) were estimated from the plasma frequencies. The obtained transfer integrals are listed in Table 1, together with the transfer integrals of other organic conductors obtained by the same procedure. The anisotropy of the transfer integral, i.e., t_2/t_1, is 0.3 in this material. This value is considerably smaller than that of α-(BEDT-TTF)$_3$(ReO$_4$)$_2$[13] or (BEDT-TTF)$_3$(ClO$_4$)$_2$,[12] but it is larger than that of (TMTSF)$_2$PF$_6$[16].

(BEDT-TTF)HgBr$_3$. Figure 4 shows the crystal structure of this salt.[9] Like other BEDT-TTF salts the BEDT-TTF molecules form conducting sheets parallel to the (010) plane; these molecules are separated from each other by the anions. The BEDT-TTF$^+$ ions in this complex are strongly dimerized, and the dimers are overlapping, with an eclipsed configuration.[9] The direction connecting the center of the two BEDT-TTF molecules within the dimer is in the (001) plane rather than in the (010) plane. Hereafter we will call this direction axis the L-axis. This axis is roughly parallel to the [$\bar{1}$10] axis. The long axis of the BEDT-TTF molecule is also roughly in the (001) plane, almost perpendicular to the L-axis. The overlap integrals between HOMO, depicted in Fig. 4, were calculated to be $a1$=39.95×10^{-3}, $a2$=−0.98×10^{-3}, c=−10.51×10^{-3}, $p2$=−0.30×10^{-3}, and $p1$=−0.08×10^{-3}, respectively. This calculation explicitly shows the strong dimerization in this salt. By using this equation t_{calc}=E·$a1$; E=10 eV, t_{calc} is calculated to be 0.39 eV within a dimer. This value is quite large as compared with the usual transfer integral in BEDT-TTF salt.

The reflectance spectra were measured on the (001) plane for the light polarization parallel and perpen-

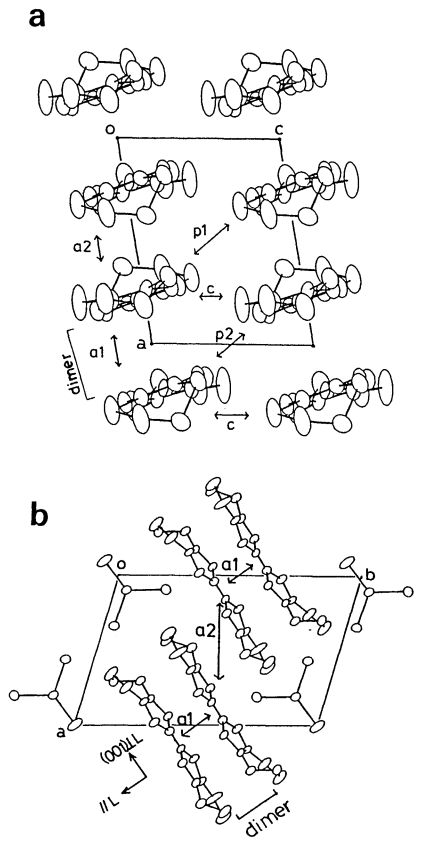

Fig. 4. (a) The crystal structure of (BEDT-TTF)$HgBr_3$ in the conducting plane. The overlap integrals between HOMO's depicted in the figure are $a1=39.95\times10^{-3}$, $a2=-0.98\times10^{-3}$, $c=-10.51\times10^{-3}$, $p2=-0.30\times10^{-3}$, and $p1=0.08\times10^{-3}$, respectively. (b) The crystal structure projected onto the ab-plane. L-axis connects the centers of two BEDT-TTF molecules within the dimer.

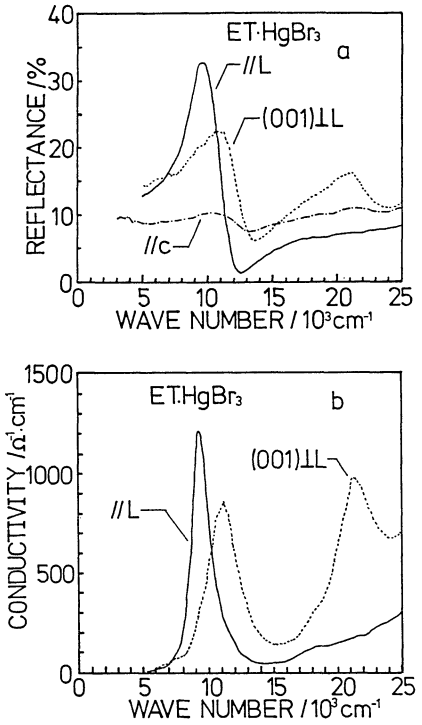

Fig. 5. (a) The reflectance spectra (//L, (001)⊥L, //c) and (b) conductivity spectrum (//L, (001)⊥L) of (BEDT-TTF)$HgBr_3$ at room temperature.

dicular to the L-axis and on the (010) plane for the polarization parallel to the c-axis. Figure 5 shows the reflectance spectra (//L, (001)⊥L, //c) and the conductivity spectra (//L, (001)⊥L) of this salt at room temperature. From the definition of the L-axis, the dispersion appearing in the //L spectrum is ascribed to the charge-transfer excitation within the dimer. On the other hand, the dispersion in the (001)⊥L spectrum is ascribed to the local excitation of BEDT-TTF^+, because the long axis of BEDT-TTF^+ is in this direction, as have been described above. This interpretation is consistent with the previously reported results on simple salts of BMDT-TTF, where local excitations at 11000 cm^{-1} and 21000 cm^{-1} were found to be polarized along the molecular long axis.[17] Since the charge-transfer excitation at 10000 cm^{-1} in the //L spectrum is close to the local excitation at 11000 cm^{-1} in the (001)⊥L pectrum, they do not separate from each other in the case of an improper choice of polarization direction. However, the inherent mixing of the charge-transfer excitation with the local excitation is not expected to appear in this salt, because the overlap of the neighboring BEDT-TTF molecule within the dimer is eclipsed; hence, the molecular plane is almost perpendicular to the L-axis.

In the //c spectrum, a weak dispersion also appears at 11000 cm^{-1}. This dispersion is ascribed to the superposition of the c-component of the CT transition within the dimer and the c-component of the local excitation along the molecular long axis. The other transition is not clearly observed in the //c spectrum. Therefore, it is concluded that the CT transition originally polarized along the c-axis is negligible in this salt in spite of the relatively large overlap integral along the c-axis ($c=-10.51\times10^{-3}$; see Fig. 4). This suggests that the electronic structure of this material is inherently described by a dimer model. Thus we can safely assume the dimer model in order to estimate the effective on-site Coulomb repulsion energy (U_{eff}) and the transfer integral (t), both of which appear in the Hubbard Hamiltonian. In this model, the plasma frequency and the peak position are described by the following equations:

$$\omega_p^2=[16\pi a^2e^2/\Omega\hbar^2]\cdot[t^2/\sqrt{U_{eff}^2/4+4t^2}], \quad (3)$$

$$\hbar\omega_{CT}=U_{eff}/2+\sqrt{U_{eff}^2/4+4t^2}, \quad (4)$$

where a, Ω, ω_{CT}, and ω_p are the distance between the molecules forming a dimer, the volume per dimer, the excitation energy, and the plasma frequency respectively. These values are $\Omega=978.8$ Å^3, $a=3.62$ Å, $\omega_{CT}=9100$ cm^{-1}, and $\omega_p=10000$ cm^{-1}, where ω_p has been calculated by integrating the conductivity spectrum from 5000 cm^{-1} to 15000 cm^{-1}. By the use of

Table 2. Comparison of U_{eff} Values Obtained in Various Complex

Structure**	(4) dimer //	(5) 1d // a	(6) 1d // c	(7) 2d // c	(7) 2d // b	(8) 1d // c
$\omega_{CT}/10^3$ cm^{-1}	10.0	4.4	5.0	4.9	8.9	11.7
a/Å	3.62	4.47	5.84	5.63	7.50	3.57
U_{eff}/eV***	0.69[d]	1.20[c]	0.57[d] (1.0[c])	0.60[d]	1.1[d]	1.25[d]
t/eV***	0.35[d]	0.22[c]	0.09[d] (0.14[c])	0.08[d]	<0.11[d]	0.28[d]
$S\times10^{-3}$	39.0	—	10.6	12.5	5.1	—

(4): (BEDT-TTF)$HgBr_3$, (5): (BEDT-TTF)$AuCl_2Br_2$,[18] (6): (BMDT-TTF)AsF_6,[17] (7): (BMDT-TTF)SbF_6,[17] (8): (TTF)$Br_{0.79}$.[19]
** 1d: one-dimensional chain structure, 2d: anisotropic two-dimensional structure. *** d: results of dimer model, c: results of linear-chain model.

this value, U_{eff} and t are estimated to be 0.69 eV and 0.35 eV respectively, by solving the Eqs. 2 and 3. The obtained value of the transfer integral is very close to the calculated value (t_{calc}=0.39 eV). Table 2 compares the U_{eff} value obtained in this study with the previously reported values. Some of the U_{eff} values in this table are those obtained by the use of the linear-chain model, while others are those obtained by the use of the dimer model. It should be kept in mind that the choice of model is not necessarily appropriate in the cases of (TTF)$Br_{0.79}$[19] and (BMDT-TTF)SbF_6.[17] The U_{eff} value of (BEDT-TTF)$HgBr_3$ is comparatively smaller than that of (BEDT-TTF)$AuCl_2Br_2$.[18] This implies an incompleteness in the description of the electronic structure due to the assumed Hubbard Hamiltonian; in other words, the nearest neighbor Coulomb interaction is non negligible in this case, as we have previously pointed out (cf. Ref. 17).

Within the framework of the dimer model, the U_{eff} in the Hubbard Hamiltonian can be exactly replaced by $U-V$ in terms of the Extended Hubbard Hamiltonian, where U and V are the on-site Coulomb interaction and the nearest neighbor Coulomb interaction respectively. Therefore, in the material with a strongly dimerized structure it is possible to analyze the optical spectrum by the use of the Extended Hubbard Hamiltonian. Hence, 0.69 eV can be taken as the exact $U-V$ value in the case of (BEDT-TTF)$HgBr_3$. Because of the strongly dimerized structure of (BEDT-TTF)$HgBr_3$, the V value could be a little larger than the corresponding values in other BEDT-TTF salts, but their difference should be small. Thus, we can consider that the $U-V$ value is about 0.7 eV in the family of BEDT-TTF salts.

Unfortunately, no exact solution has yet been established for the linear-chain Extended Hubbard model. Although the analysis based on the linear-chain Hubbard model is no longer applicable when we take the Extended Hubbard Hamiltonian, it may be used for a qualitative discussion. As we have pointed out in Ref. 17, the value of $U-V$ in the material with a linear-chain structure can be expected to be larger than the U_{eff} value obtained by the use of the dimer Hubbard model and smaller than the U_{eff} value obtained by the use of the linear-chain Hubbard model. This is consistent with the fact that the U_{eff} in the (BEDT-TTF)$AuCl_2Br_2$[18] obtained by the use of the linear-chain model is considerably larger than the $U-V$ value estimated in this study.

The value of $U-V$ was found to be between 1 and 0.6 eV[17] in the case of the BMDT-TTF salt; this is comparable to the corresponding value in the BEDT-TTF salt. On the other hand, the U_{eff} of (TTF)$Br_{0.97}$ estimated by the use of the dimer model was 1.25 eV.[19] Since this material has a uniform structure, the value mentioned above gives the lowest limit of the $U-V$ value. Therefore, we can consider that the $U-V$ value is smaller in BEDT-TTF and BMDT-TTF salts than in TTF salts. This smallness of the $U-V$ value may be the origin of the frequent appearance of type-A in the family of BEDT-TTF salts.

Summary and Conclusion

In this paper we reported on the reflectance spectra of (BEDT-TTF)$_5Hg_3Br_{11}$, and (BEDT-TTF)$HgBr_3$. In the former salt, spectral change due to the metal-insulator transition is observed at 100 K below 1000 cm^{-1}. The ratio of transfer integrals perpendicular and parallel to the [$\bar{1}$02] axis is estimated to be 0.3. In the latter salt, we found that $U_{eff}=U-V=0.69$ eV, and t=0.35 eV by the use of dimer model. The value of $U-V$ in the BEDT-TTF family is comparable to that of the BMDT-TTF family, but considerably smaller than the corresponding value in the TTF family.

We wish to thank Prof. Kyuya Yakushi for his valuable discussion. We also appreciate the generous gift of d_8-BEDT-TTF by Prof. Gunzi Saito and Dr. Hatsumi Mori. This work was supported by Grants-in-Aid for the Encouragement of Young Scientists (No. 01740259) and for Scientific Research (No. 01470004) from the Ministry of Education, Science and Culture.

References

1) *Synth. Met.*, **27**, No 1,2 (1988).
2) a) I. D. Parker, D. D. Pigram, R. H. Friend, M.

Kurmoo, and P. Day, *Synth. Met.*, **27**, A387 (1988); b) K. Murata, N. Toyota, Y. Honda, T. Sasaki, M. Tokumoto, H. Bando, H. Anzai, Y. Muto, and T. Ishiguro, *J. Phys. Soc. Jpn.*, **57**, 1540 (1988); c) K. Oshima, T. Mori, H. Inokuchi, H. Urayama, H. Yamochi, and G. Saito, *Phys. Rev. B*, **38**, 938 (1988); d) M. V. Kartsovnik, V. N. Laukhin, V. I. Nizhankovskii, and A. A. Ignatev, *JETP. Lett.*, **47**, 363 (1988).

3) a) H. Tajima, H. Kanbara, K. Yakushi, H. Kuroda, and G. Saito, *Solid State Commun.*, **57**, 911 (1986); b) M. Tamura, K. Yakushi, H. Kuroda, A. Kobayashi, R. Kato, and H. Kobayashi, *J. Phys. Soc. Jpn.*, **57**, 3239 (1988); c) A. Ugawa, G. Ojima, K. Yakushi, and H. Kuroda, *Phys. Rev. B*, **38**, 5122 (1988).

4) T. Mori and H. Inokuchi, *J. Phys. Soc. Jpn.*, **57**, 3674 (1988).

5) H. Kuroda, K. Yakushi, H. Tajima, A. Ugawa, M. Tamura, Y. Okawa, A. Kobayashi, R. Kato, H. Kobayashi, and G. Saito, *Synth. Met.*, **27**, A491 (1988).

6) K. Yakushi, S. Aratani, K. Kikuchi, H. Tajima, and H. Kuroda, *Bull. Chem. Soc. Jpn.*, **59**, 363 (1986).

7) S. Mazumdar and A. N. Bloch, *Phys. Rev. Lett.*, **50**, 207 (1983).

8) G. Saito, T. Enoki, K. Toriumi, and H. Inokuchi, *Solid State Commun.*, **42**, 557 (1982).

9) T. Mori, P. Wang, K. Imaeda, T. Enoki, and H. Inokuchi, *Solid State Commun.*, **64**, 733 (1987).

10) Y. Iyechika, K. Yakushi, H. Kuroda, and G. Saito, *Solid State Commun.*, **49**, 769 (1984).

11) H. Tajima, K. Yakushi, H. Kuroda, and G. Saito, *Solid State Commun.*, **49**, 769 (1984).

12) H. Tajima, H. Kanbara, K. Yakushi, H. Kuroda, G. Saito, and T. Mori, *Synth. Met.*, **25**, 323 (1988).

13) K. Yakushi, H. Kanbara, H. Tajima, H. Kuroda, G. Saito, and T. Mori, *Bull. Chem. Soc. Jpn.*, **60**, 4251 (1987).

14) We also observed the local excitation of BEDT-TTF^{2+} in $(BEDT\text{-}TTF)_3(MnCl_4)_2$ at almost the same wavenumber (unpublished results).

15) For this procedure of analysis, see C. S. Jacobsen, J. M. Williams, and H. H. Wang, *Solid State Commun.*, **54**, 937 (1985).

16) C. S. Jacobsen, D. B. Tanner, and K. Bechgaard, *Phys. Rev. Lett.*, **53**, 194 (1984).

17) M. Yoshitake, K. Yakushi, H. Kuroda, A. Kobayashi, R. Kato, and H. Kobayashi, *Bull. Chem. Soc. Jpn.*, **61**, 1115 (1988).

18) A. Ugawa, K. Yakushi, and H. Kuroda, National Meeting of the Chemical Sciety of Japan, Tokyo, March **1981**, Abstr., No3ICO1.

19) J. B. Torrance, B. A. Scott, B. Welber, F. B. Kaufman, and P. E. Seiden, *Phys. Rev. B*, **19**, 730 (1979).